

# Parametric Study of Single-Span Jointless Steel Bridges

HEMANATH K. THIPPESWAMY, PENMATSARAJU, AND HOTA V. S. GANGARAO

An engineering explanation for the performance of single-span jointless steel bridges is presented. The performance of jointless bridges is shown to depend on the ratio of superstructure to substructure stiffness, including span length and abutment heights, load types and their combinations, time-dependent creep effects, foundation types, soil properties, and boundary conditions. A finite element analysis program was used to generate moment and deformation data, and the data were then synthesized to develop a better understanding of jointless bridge behavior. The moment and deformation data were also generated for a simply supported jointed bridge to compare with a jointless bridge. The results are presented and discussed for various loading conditions and load combinations. The results of the parametric study serve as a guide to select superstructure and substructure sizes and also to provide a tool for structural optimization. The study found that maximum midspan moment caused by external loads, including time-dependent loads such as creep and shrinkage in a jointless bridge, is about 50 percent of the maximum midspan moment found in a simply supported jointed bridge. The lower midspan moment in a jointless bridge as a result of a combination of all loads explains the superiority of the performance of a jointless bridge over a simply supported jointed bridge. The study also found that the effect of soil settlement and earth pressure is minimal when the jointless bridge has a hinged type of boundary condition at the footing level.

Jointed bridges are extremely common in bridge construction and share about 98 percent of total bridges (1,2). Joints are provided to accommodate longitudinal movements in bridges. Longitudinal movements are caused by thermal changes, horizontal earth pressure, soil settlements, and braking forces. Depending on the type of superstructure, span length, and boundary conditions of the bridge, different types of expansion joints and bearings are used in the field. Despite extensive research on expansion joints and bearings, researchers (3) have observed that expansion joints and bearings do not serve their intended purpose. In many instances, the major problems in joints and bearings (typical in the case of open joints, sliding plate joints, and open finger joints) encountered are

- Corrosion caused by deicing chemicals leaking through the joints,
- Accumulation of debris and other foreign material restricting the free joint movement,
- Differential elevation at the joints causing additional impact forces, and
- High initial and maintenance costs of joints and bearings.

These problems can lead to costly repair and rehabilitation of jointed bridges. To reduce the cost of bridge maintenance and improve the structural efficiency, transportation departments of vari-

H. K. Thippeswamy and H. V. S. GangaRao, Constructed Facilities Center, West Virginia University, Morgantown, W. Va. 26506-6101. P. R. Raju, Michael Baker, Jr., Inc., 420 Rouser Rd. Coraopolis, Pa. 15108.

ous states in the United States have tried to build bridges without joints and bearings. This new approach of integrating bridge superstructure with the abutments and piers has been adopted by as many as 28 states in the United States, with Tennessee taking the lead (4). Such a class of bridges is referred to as jointless or integral bridges.

Engineers have observed that integral bridges are performing better than jointed bridges with reduced initial and life cycle costs and also with minimal maintenance problems. Construction of integral bridges is simpler and faster than the construction of jointed bridges because they require fewer parts and less material and are less labor intensive (5). Conversion of simply supported bridges into integral bridges has been successful and has been shown to improve the performance of the bridge. The field performance of existing jointless bridges has been well documented by many researchers (4-10). Integral bridges also have performed better under earthquake forces than bridges with joints because the continuity between superstructure and substructure develops higher energy dissipation (11).

During the design of integral bridges, attention must be given to the following: (a) gravity and environmental loads (5); (b) settlement, temperature variations, and earth pressure (4); and (c) stability of superstructure and substructure during construction and service. Special attention is required for integral bridges when they are built on skew and curves. The joint between the superstructure and abutment has to be carefully designed and detailed to resist the support moment at the joint by limiting the concrete crack width to avoid reinforcement or steel corrosion.

## RESEARCH NEEDS

In spite of the many advantages of jointless bridges over jointed bridges, large numbers of new jointless bridges are not being built and large numbers of jointed bridges are not being converted to jointless bridges. The reasons may be attributed to the following:

- An inadequate understanding of integral bridge behavior under soil settlement, temperature, and earth pressure;
- Limited performance data;
- Inadequate experimental and analytical evaluations;
- A lack of design and construction specifications; and
- A higher cost to convert jointed bridges to jointless bridges.

The design criteria are empirical and are based on observations of the performance of few in-service jointless bridges. For jointless bridges, design and construction specifications are not yet included in AASHTO's Specifications for Highway Bridges (12). Consequently, variations in the analysis and design are found from state to state. To properly understand the behavior of integral bridges, analytical data must be developed and carefully interpreted. As a

minimum, the following parameters play an important role and should be studied to predict the behavior and performance of integral bridges:

- Effects of superstructure and substructure stiffness in the design of jointless bridges;
- Effects of concrete creep and shrinkage, temperature, and soil settlement in the design of jointless bridges;
- Effect of varying soil properties, types of foundation, and connection details between the foundation and the abutment; and
- Effect of approach slab and its connection with the jointless bridge.

## OBJECTIVES

The primary objective of this paper is to present the response of single-span jointless steel bridges by varying the ratios of superstructure to substructure stiffness, load types and their combinations, foundation types, soil properties, and boundary conditions and also to study the time-dependent creep effects of superstructural material on jointless bridge behavior. An additional objective is to explain the superior performance of a jointless bridge over a jointed bridge, particularly in terms of accommodating longitudinal thermal movements.

## SCOPE

Research is being conducted at West Virginia University to study the effect of various loads and their combination, including thermal load, earth pressure and soil settlement, spans, heights, foundation types, soil properties, and abutment stiffness. The study addresses the reason for better performance of jointless bridges over jointed bridges. The finite element method that treats the bridge structure as a plane frame has been used to develop data and perform the parametric study on jointless bridge structures. In earlier studies (13), due consideration was not given to many influencing parameters, such as superstructure and substructure stiffness ratio, span length, abutment/pier height, and different boundary conditions. Results obtained in the parametric study were compared with those obtained from the simple frame formulas (14). The influence of various parameters on bridge behavior is discussed with the help of graphs and tables. Results of time-dependent creep analysis is also presented for one case of a jointless bridge.

## PARAMETERS CONSIDERED

Effects of variation in span length, abutment height, ratio of superstructure to substructure stiffness, gravity load, environmental load (temperature), horizontal load (earth pressure and braking), soil settlement, and their combinations have been studied in terms of jointless bridge response. Three types of boundary conditions are considered: hinged, fixed, and partially fixed. Partially fixed boundary conditions are represented by means of rotational springs. Three values are assumed for these rotational springs to represent different types of soils and foundations. Additional details are given in the following sections.

## Span Length

The span lengths ( $L$ ) varied in the parametric study were 9.2, 15.3, 22.9, and 30.5 m (30, 50, 75, and 100 ft). The geometric property of the superstructure was arrived at by considering the full composite action of concrete slab with steel stringer. The moment of inertia ( $I_s$ ) of the superstructure was arrived at by satisfying the maximum allowable deflection criterion of  $L/800$ . The superstructure was made of a cast-in-place or a precast concrete bridge deck built composite with steel stringers.

## Abutment Height

The abutments were considered to be made of reinforced concrete for varying heights ( $H$ ), that is, 3.1, 6.1, 12.2, and 18.3 m (10, 20, 40, and 60 ft). The moment of inertia ( $I_c$ ) of the abutment was varied from 0.2 to 3 times the moment of inertia of the superstructure.

## Ratios of Superstructure to Substructure Stiffness

The ratio of superstructure moment of inertia and substructure moment of inertia was varied from 0.3 to 5. The ratio of superstructure to substructure stiffness is a nondimensional parameter represented by stiffness ratio  $K = (H/L) (I_s/I_c)$ . The stiffness ratio was varied from 0.1 to 3, which represents a wide range of practical field cases of jointless bridges.

## Gravity Loads

The dead and live loads were considered in the design of concrete deck and steel stringers. The dead load included the weight of slab, wearing surface, parapets, railings, curbs, haunches, and diaphragms. The design live load was arrived at according to AASHTO specifications (12). The effect of multiple lanes, wheel load distribution, and impact were also considered in arriving at the maximum design live load.

## Horizontal Loads

Horizontal loads are caused by earth pressure and braking force. Earth pressure is assumed to act on one side of the frame, which is a critical case. The Rankine's coefficient of active earth pressure is considered for granular type of backfill, which is commonly adopted (15). The total earth pressure is computed using Rankine's theory of active earth pressure, and the total load is assumed to be applied at one-third the height of the abutment from the top of the foundation. The braking force is calculated and applied according to AASHTO specifications (12).

## Environmental Load (Temperature)

A linear temperature gradient across the depth is assumed to act on the deck and girder system of the jointless bridge model. The temperature gradient varied from 38°C (100°F) at the top of the deck to 21°C (70°F) at the bottom of the stringer. The reference temperature is assumed to be 21°C (70°F). The temperature is selected on

the basis of the AASHTO specifications (12) for concrete temperature rise in a moderate climate. The temperature gradient is accounted for in the superstructure design only. The coefficient of thermal expansion used is  $6 \times 10^{-6}$  in./in./°F as specified for concrete by AASHTO (12).

### Differential Settlement of Soil

The differential settlement of abutments is assumed to be 13, 25, 51, and 330 mm ( $\frac{1}{2}$ , 1, 2, and 3 in.). These discrete values for settlement are considered to simplify the problem of time-dependent settlement of the supporting soil and to establish the tolerable differential settlement limit.

### Boundary Conditions

A realistic boundary condition for jointless bridges at foundation level would be somewhere between hinged and fixed conditions, depending on the type of footing and the soil media. Therefore, hinged and fixed (extreme cases) and partially fixed boundary conditions are considered in the parametric study of single-span jointless steel bridges. The partial fixity is achieved in jointless bridge parametric study by providing rotational springs between the abutment and the foundation. Three spring constants [4.6E10, 9.2E10, and 3.5E11 kg-mm/rad (4E9, 8E9, and 30E9 lb-in./rad)] are assumed for partially fixed boundary conditions on the basis of the type of foundation and supporting soil.

### Creep and Shrinkage

Time-dependent creep analysis (16) under sustained dead load has been conducted for a 15.3-m (50-ft) jointless bridge under consideration. The creep-induced moments are calculated for 10 years.

**TABLE 1 Moments for Example Jointed Bridge Under Consideration**

LOAD CASE	JOINTED (SIMPLY SUPPORTED) BRIDGE WITH FIXED CONDITION AT ABUTMENT BASE			
	SUPERSTRUCTURE MOMENT (t-m)		ABUTMENT MOMENT (t-m)	
	MIDSPAN	SUPPORT	TOP OF ABUT.	BOTTOM OF ABUT.
LIVE LOAD	87	0	0	0
DEAD LOAD	56	0	0	0
EARTH PRESSURE	0	0	0	-42
TEMPERATURE	0	0	0	0
SETTLEMENT (1")	0	0	0	0
BRAKING	0	0	0	-7
CREEP	0	0	0	0
SHRINKAGE	0	0	0	0
TOTAL	143	0	0	-49

Note: 1 kip-ft = 0.1385 t-mt

The analysis was conducted for creep in the superstructure only. The creep coefficient and the aging coefficient adopted in the analysis are 2.3 and 0.7, respectively. The results of creep analysis are shown in Tables 1 and 2.

Shrinkage analysis was conducted for a 15.3-m (50-ft) jointless bridge (16). The shrinkage-induced moments were found for the superstructure at 10 years.

### SINGLE-SPAN MODEL

A single-span jointless bridge is modeled as a two-dimensional frame by varying the stiffness ratio of the superstructure and the substructure and boundary conditions. The deck and the stringers are modeled as one-dimensional beam elements assuming full com-

**TABLE 2 Moments for Example Jointless Bridge Under Consideration**

LOAD CASE	JOINTLESS BRIDGE WITH HINGED-HINGED CONDITION AT ABUTMENT BASE				JOINTLESS BRIDGE WITH FIXED-FIXED CONDITION AT ABUTMENT BASE			
	SUPERSTRUCTURE MOMENT		ABUTMENT MOMENT		SUPERSTRUCTURE MOMENT		ABUTMENT MOMENT	
	MIDSPAN	SUPPORT	TOP OF ABUT.	BOTTOM OF ABUT.	MIDSPAN	SUPPORT	TOP OF ABUT.	BOTTOM OF ABUT.
LIVE LOAD	54.3	-31.8	-31.8	0	52.0	-34.3	-34.3	16.9
DEAD LOAD	28.0	-28.0	-28.0	0	26.3	-29.8	-29.8	14.7
EARTH PRES.	-2.2	-18.0	-18.0	0	-0.8	1.8	1.8	-29.4
TEMP.	15.9 (-15.9)	15.9 (-15.9)	15.9 (-15.9)	0	16.2 (-16.2)	16.2 (-16.2)	16.2 (-16.2)	2.4 (-2.4)
SETT. (1")	0	0	0	0	0	-20.8	-20.8	-20.8
BRAKING	0	5.0	5.0	0	0	1.9	1.9	-3.2
CREEP	-3.1	-3.1	-3.1	0	-3.2	-3.2	-3.2	2.1
SHRIN.	-14.1	-14.1	-14.1	0	-17.4	-17.4	-17.4	3.6
TOTAL	78.8 (47.0)	-74.1 (-105.9)	-74.1 (-105.9)	0	73.1 (40.7)	-85.6 (-118.0)	-85.6 (-118.0)	-18.5 (-13.7)

Note: 1 kip-ft = 0.1385 t-m; Numbers in the brackets account for winter temperature gradient.

posite action. ANSYS STIF 3 (17) beam element is used with 4 degrees of freedom at each node of the element. Partial fixity is simulated by using ANSYS STIF 14 (17) spring-damper element, wherein the effect of the damper is suppressed suitably in the input code by giving a zero value for damping coefficient. All the loads are prescribed as individual load cases and the inputs are given accordingly in the ANSYS input data file. Analysis is carried out for each span varying all the parameters discussed above. The results obtained from the ANSYS program were compared with those from other analytical methods (14) and found to be correlating with an error of less than 0.5 percent.

## RESULTS OF PARAMETRIC STUDY

The results of the parametric study for single-span jointless bridges are summarized in the form of graphs (Figures 1 through 12). Different loads, stiffness ( $K$ ) values, and boundary conditions were varied in the parametric study. The most important results of the parametric study are discussed herein.

### MOMENT AT FOUNDATION LEVEL

Figures 1 through 4 show the moment variation for various boundary conditions at foundation level for varying stiffness ratios. Figures 1 through 4 are developed for live load, environmental load, earth pressure, and various settlement, respectively. The live load

moment variation for various system stiffness ratios and for various boundary conditions is shown in Figure 1. The maximum moment of footing level is induced in the case of a fixed boundary condition, when the stiffness ratio is about 0.5. For other stiffness ratios, the moment at the footing level is small. The dead load induced moments also showed a similar trend as exhibited by live load moments. The moment values corresponding to partially fixed conditions lie in between hinged and fixed conditions. Figure 2 indicates that the smaller the stiffness ratio  $K$ , the larger is the thermally induced moment at the foundation level. Smaller system stiffness  $K$  represents a stiffer abutment and a weaker superstructure. Stiffer abutments resist a larger support moment, thereby transferring a lesser moment to the superstructure. A larger moment at support implies a larger moment at footing level for all boundary conditions except a hinged condition for thermal load (Figure 2). It is obvious and expected that the moment developed at the footing level for hinged condition should be 0 and is observed in Figures 1 through 4 for all values of stiffness ratios  $K$  and for all types of loads. Thus, the hinge type of boundary condition at the footing level would not develop undesirable moments that are to be transferred to the soil in the service life of the jointless bridge. The moment at the footing level caused by earth pressure for various boundary conditions is the highest for a system stiffness ratio of 3 (Figure 3) and low for other system stiffness ratios. The moment at the left footing caused by 1-in. settlement of the right footing is shown in Figure 4. The increase in settlement directly increases the magnitude of moment for all boundary conditions except for the hinged boundary condi-

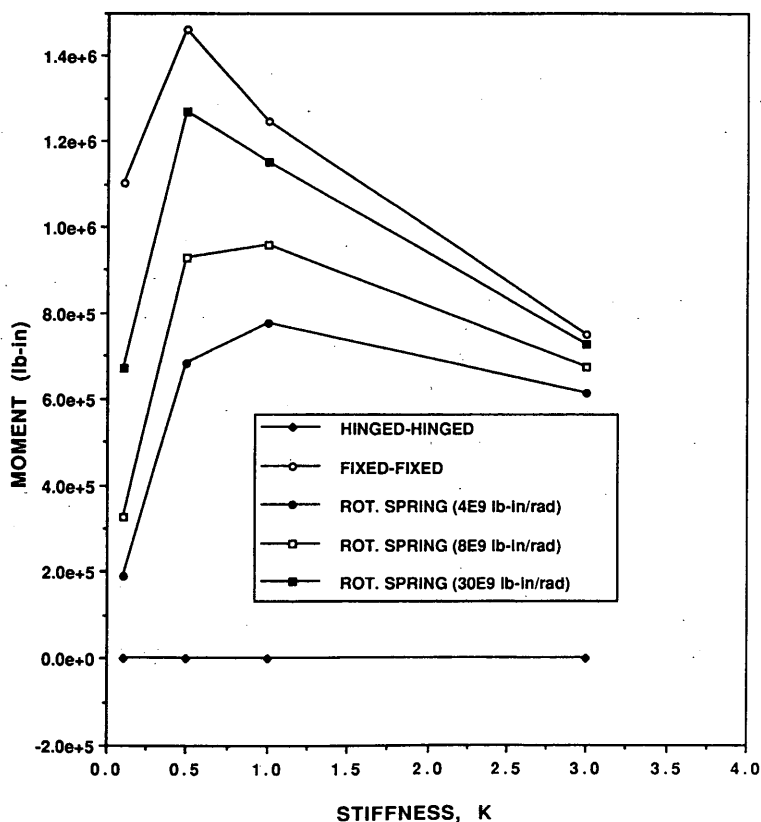


FIGURE 1 Stiffness versus moment at footing due to live load.

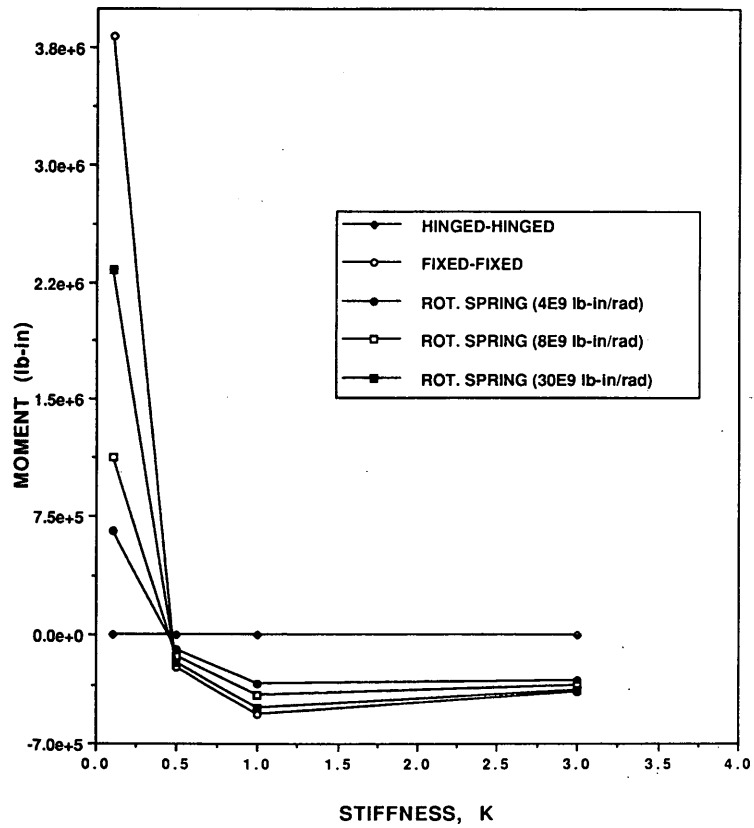


FIGURE 2 Stiffness versus moment at footing due to temperature gradient.

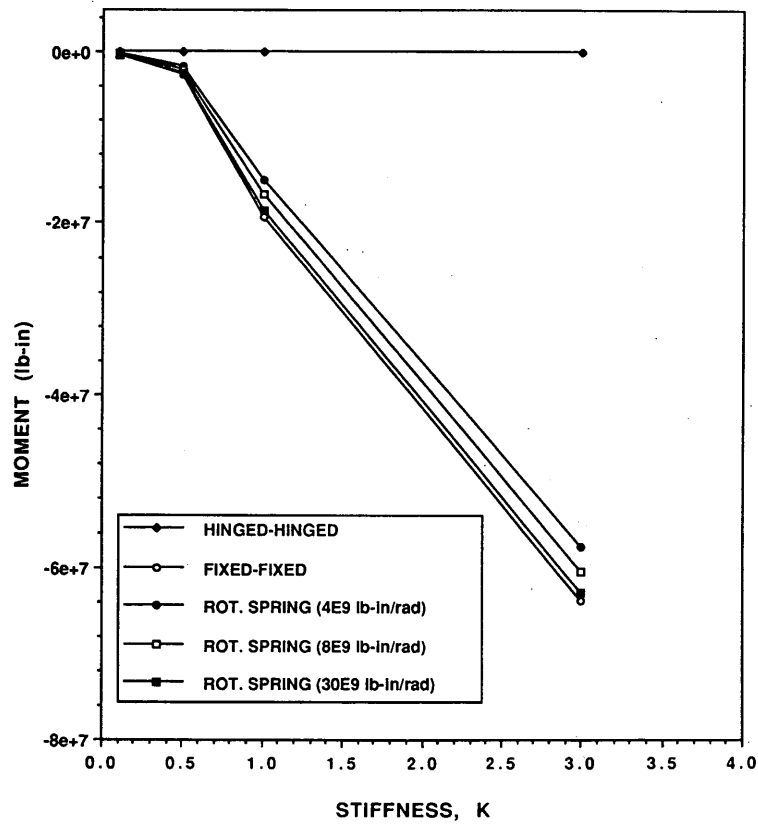


FIGURE 3 Stiffness versus moment at left footing due to earth pressure.

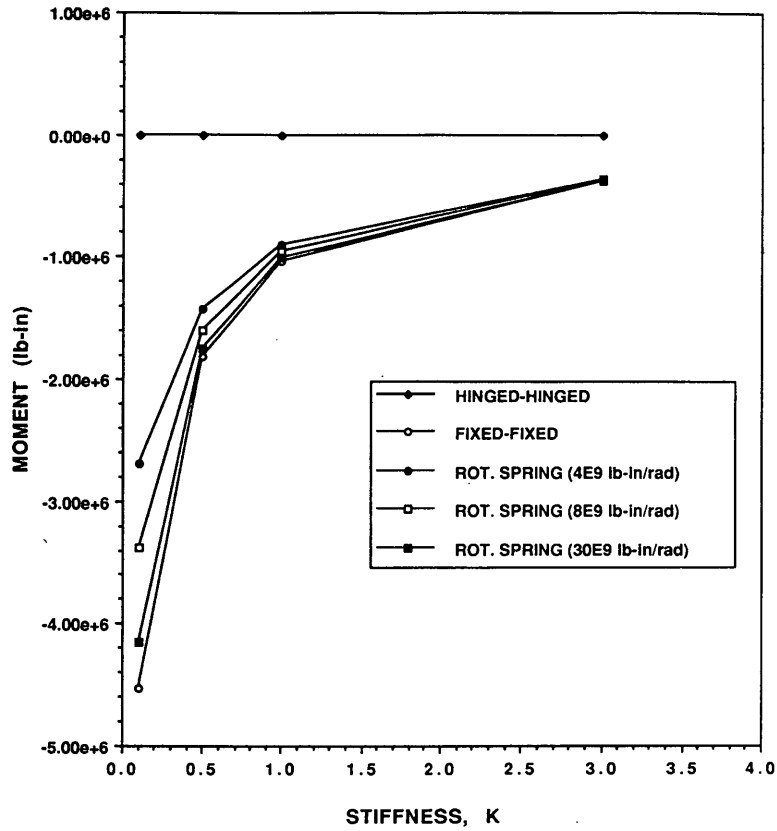


FIGURE 4 Stiffness versus moment at left footing due to settlement of 1 in. at right footing.

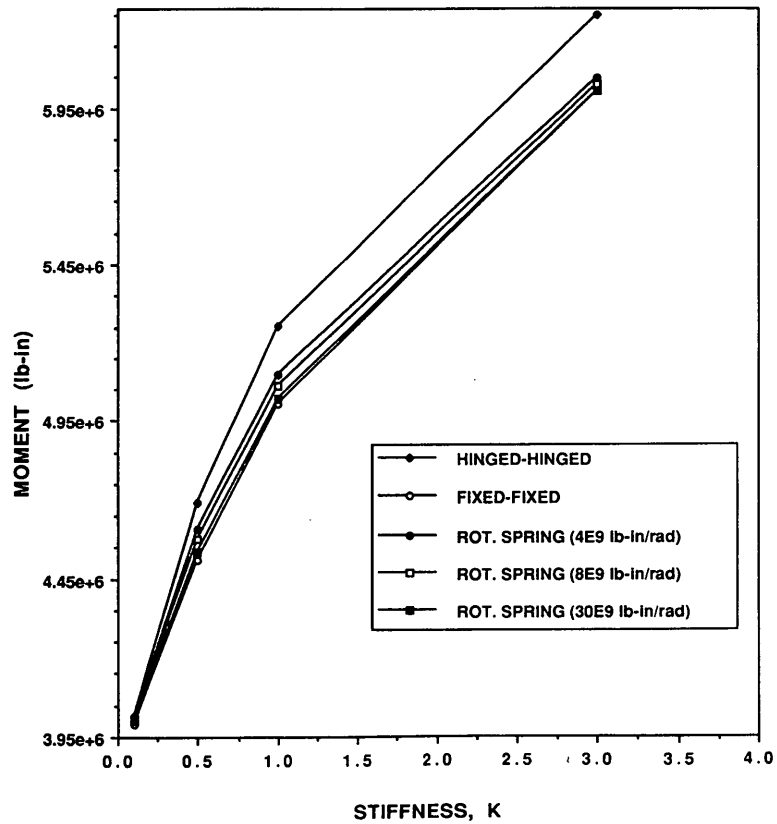


FIGURE 5 Stiffness versus moment at midspan due to live load.

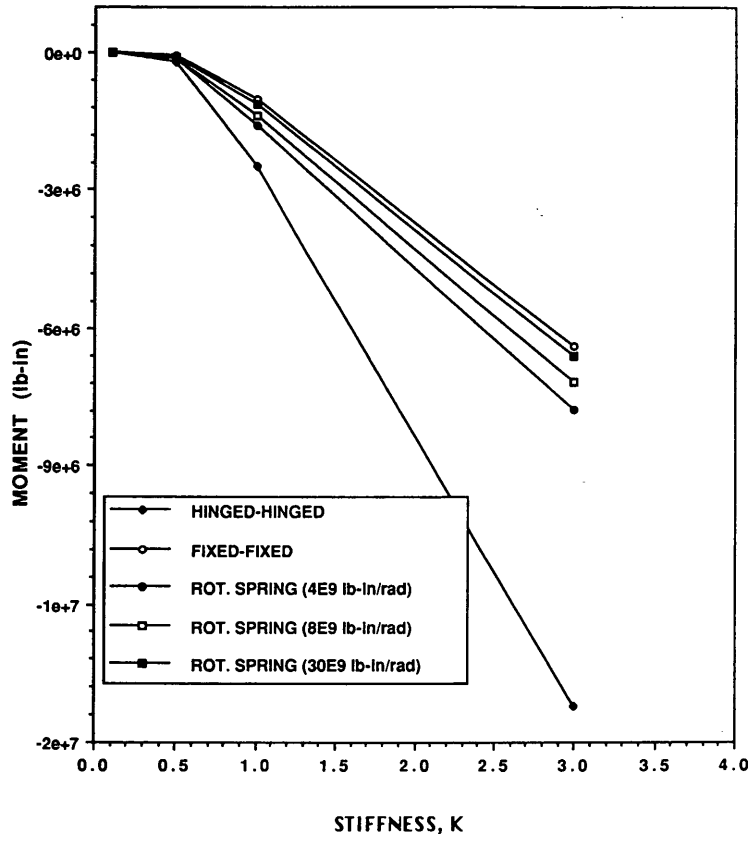


FIGURE 6 Stiffness versus moment at midspan due to earth pressure.

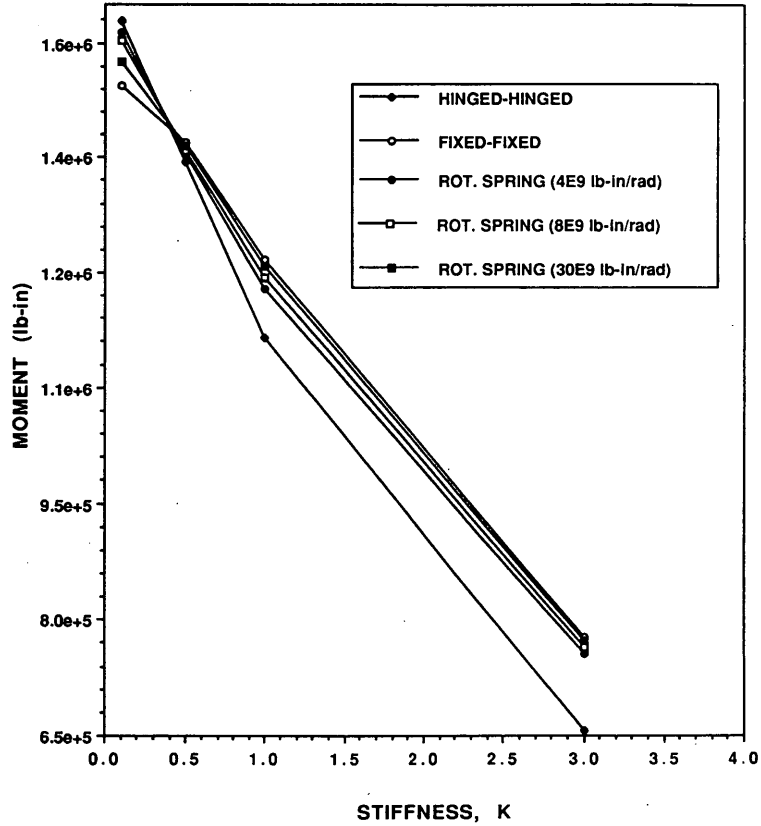


FIGURE 7 Stiffness versus moment at midspan due to temperature gradient.

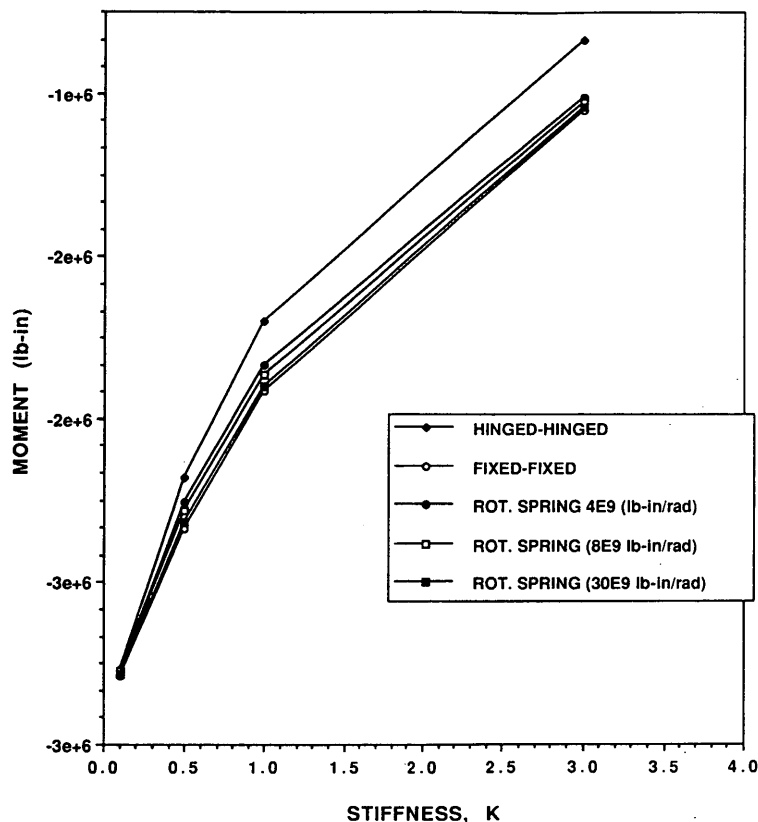


FIGURE 8 Stiffness versus moment at support due to live load.

tion; in addition, the settlement moment at the footing level is higher for a lower stiffness ratio ( $K$ ).

#### Moment at Midspan

The effect of higher  $K$  would lead to a greater midspan moment in the case of a live load and earth pressure, as indicated in Figures 5 and 6. A similar trend is observed for dead load case. The moment developed as a result of earth pressure causes tension at the top and will reduce the net moment when acting in combination with dead and live loads. Moment caused by temperature gradient at midspan is smaller for increased  $K$  values (Figure 7). An increase in stiffness ratio ( $K$ ) indicates stiffer superstructure and weaker abutment. The stiffer superstructure results in a lower midspan moment. Soil settlement moments are negligible at midspan, and the stiffness ratio  $K$  value has little effect on settlement moments.

#### Moment at Support (Superstructure and Abutment Joint)

The support moment decreases with an increase in  $K$  for live load (Figure 8). A similar trend is also observed for the dead load case. The support moment as a result of earth pressure is higher in the case of a hinged-hinged support condition and lower for other boundary conditions as shown in Figure 9. The temperature gradient produces a uniform moment throughout the superstructure. The moment

direction and magnitude at midspan and support are the same and can be seen in the Figures 7 and 10. Further, the moment at the left support is the same as the moment at the left footing level in the case of 1-in. settlement of right footing for all boundary conditions.

#### Horizontal Reaction Due to Earth Pressure

In the parametric study, the height of abutment varied from 3.1 to 18.3 m (10 to 60 ft). The total horizontal force due to earth pressure corresponding to 3.1 to 18.3 m (10 to 60 ft) in height ranged from 4994 to 181 600 kg (11 to 400 kips). Because of this wide range of lateral force associated with earth pressure, it becomes important to study the effect of earth pressure on abutment and superstructure for varied abutment and superstructure stiffness ratio ( $K$ ). The earth pressure effect on the abutment is indicated in Figure 11. The horizontal reaction caused by earth pressure is smaller at lower values of  $K$  and has an increasing trend for increasing  $K$  values. The horizontal reaction is 1.5 to 2 times higher for hinged cases over fixed cases for all values of  $K$ . The study provides useful information in deciding the system stiffness and boundary conditions to keep the horizontal reaction at a minimum.

#### Vertical Reaction Due to Earth Pressure

The vertical reactions due to earth pressure are higher for hinged boundary conditions than for fixed or partially fixed conditions. The

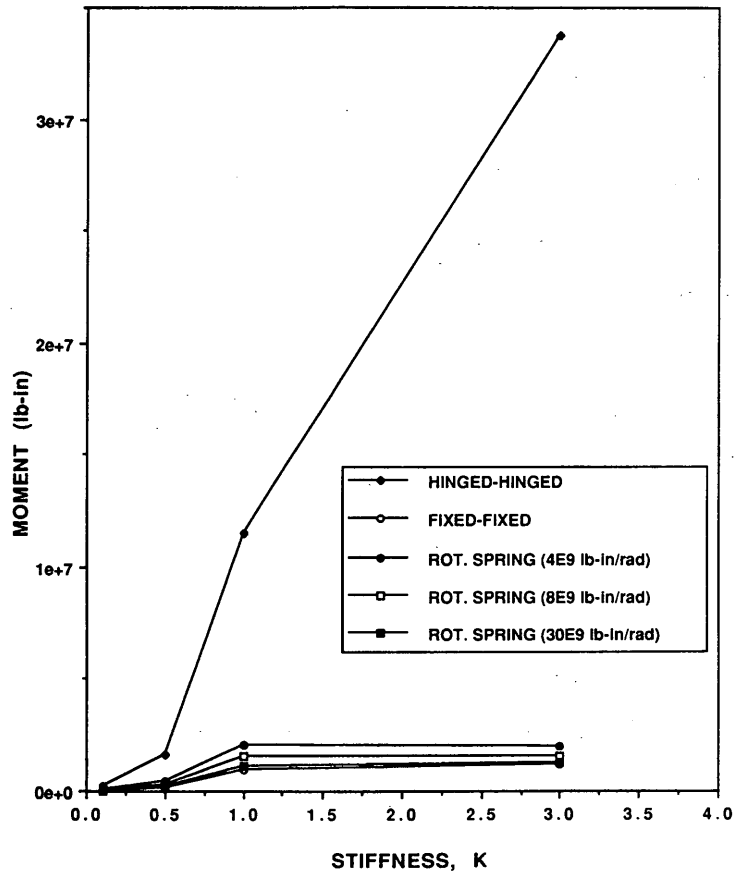


FIGURE 9 Stiffness versus moment at support due to earth pressure.

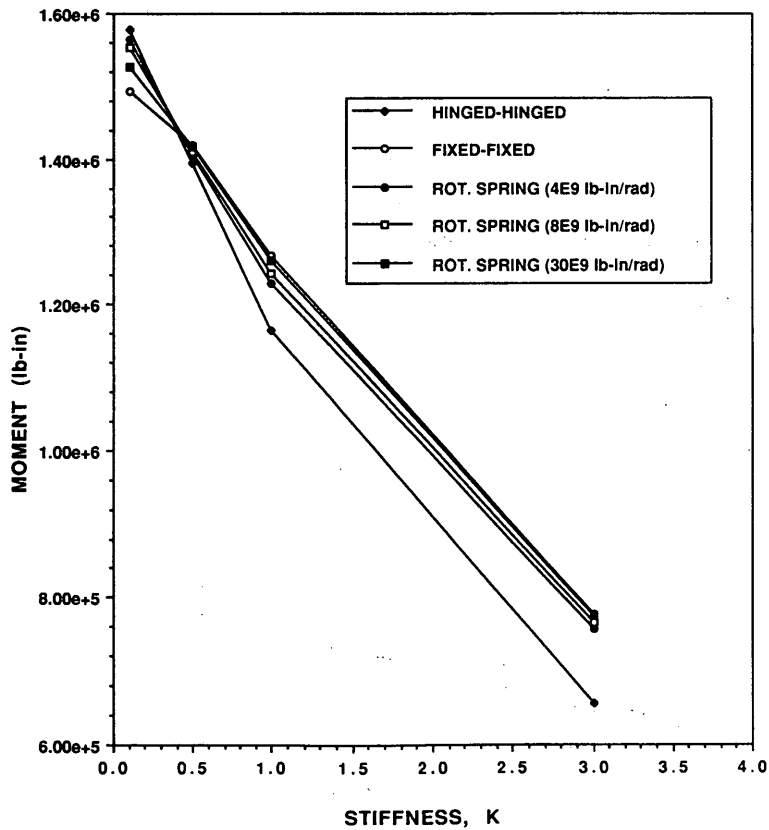


FIGURE 10 Stiffness versus moment at support due to temperature gradient.

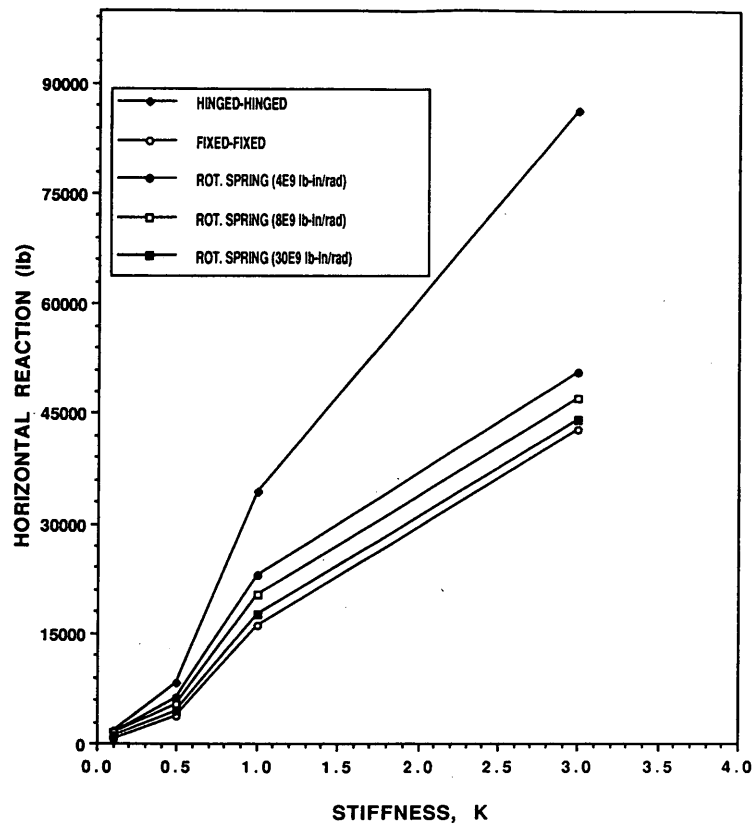


FIGURE 11 Stiffness versus horizontal reaction at right footing due to earth pressure.

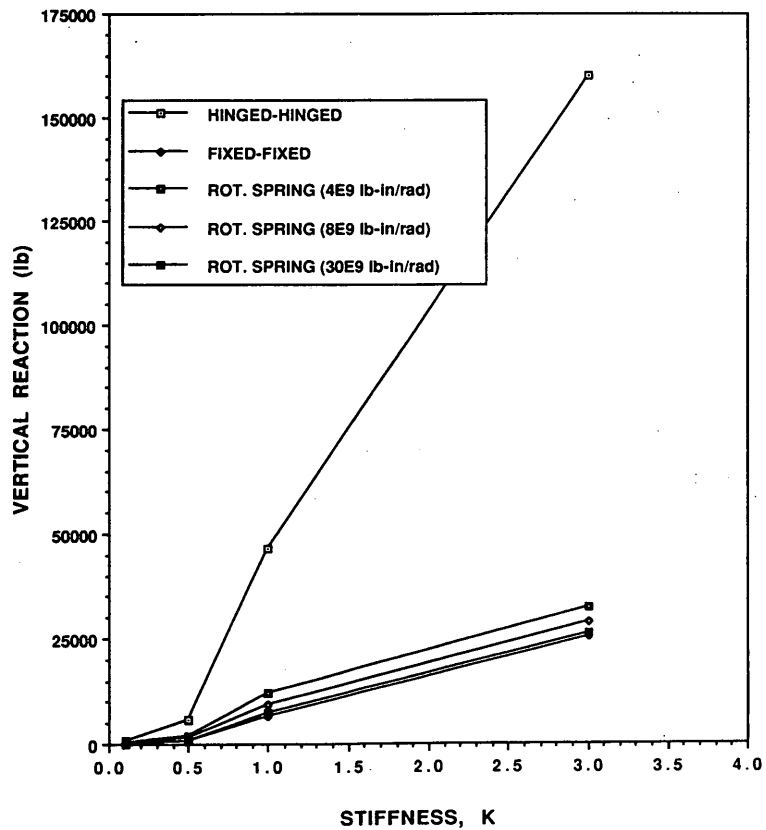


FIGURE 12 Stiffness versus vertical reaction at left/right footing due to earth pressure.

vertical reactions are about 7 to 8 times higher in hinged conditions than in other types when the stiffness ratio  $K$  is 3 (Figure 12). This large variation of vertical reactions could lead to differential settlement for large abutment heights.

### JOINTLESS BRIDGE VERSUS JOINTED BRIDGE

From the results of the parametric study, a case of a jointless bridge with a system stiffness ratio  $K$  of 0.5, a superstructure-to-substructure moment of inertia ratio of 1.25, a span length of 15.3 m (50 ft), and an abutment height of 6.1 m (20 ft) is considered to compare the results with a simply supported jointed bridge with its abutment fixed at the base. Two types of boundary conditions—hinged and fixed—are considered for the jointless bridge. Various load types are applied and the moment developed at the midspan, superstructure, and substructure joint and at foundation level is evaluated. Similar load combination effects in terms of moment are evaluated for a simply supported jointed bridge case, and the results are shown in Tables 1 and 2. In addition, the time-dependent creep-induced moment is also considered in arriving at the total moment. The superstructure and abutment are assumed to act independently in the case of the jointed bridge. The salient points are presented.

- The net moment developed at midspan during summer in a jointed bridge is found to be 1.8 and 1.9 times greater than that of the net moment developed in a jointless bridge for hinged and fixed boundary conditions, respectively. During winter, the net moment at midspan of a jointed bridge is found to be nearly 3 and 3.5 times greater than that of the net moment developed in a jointless bridge for hinged and fixed boundary conditions, respectively. The lower midspan moment in a jointless bridge caused by the combination of all loads explains the superiority of the performance of a jointless bridge over a simply supported jointed bridge.

- The moment transferred to the foundation is 0 when the jointless bridge has a hinged type of boundary condition. Therefore, the foundation and the supporting soils are less vulnerable to soil deformation in the case of a jointless bridge with a hinged type of boundary condition. The moment transferred to the foundation in a jointless bridge with fixed boundaries is 0.3 to 0.4 times that of the moment at the foundation of a simply supported jointed bridge. In the field, the support condition falls between these two extreme cases (partial fixity) and may approach a condition as that of hinged condition with time. So, a choice has to be made about the degree of fixity that may be required at the foundation of a jointless bridge. In addition, orienting the weak axes of the piles normal to traffic flow will further reduce the stresses in the piles and the soils.

- The rigid joint between the superstructure and substructure in the case of a jointless bridge is subjected to high moment, which is nearly the same as that of midspan moment. It becomes necessary to provide adequate section and proper design at the joint.

- Furthermore, connecting the approach slab to the rigid joint will further help redistribute the moment, and the joint may be subjected to a lower moment. A jointless bridge with approach slab may reduce the flexibility against horizontal movement. However, pressure relief methods have been adopted (4) to induce flexibility into the system. In a jointless bridge, the backfill seepage has a detrimental effect in terms of weakening the rigid joint and also enhancing the settlement of the approach slab. Provision of a proper drainage system will minimize the effects of backfill seepage.

- For a jointless bridge, the effect of uniform temperature (direct expansion or contraction) on the superstructure of span 15.3 m (50 ft) and height 6.1 m (20 ft) is negligible in terms of the amount of horizontal displacement of the system. However, for longer spans this may be a controlling factor.

### CONCLUSIONS

The system stiffness ratio  $K$  and the boundary conditions have significant influence on the magnitude of the moments developed in the jointless bridges. The moment at the footing associated with live and dead load is maximum when  $K$  is about 0.5. The thermally induced moment at the footing is larger for smaller  $K$  values. The moment at the footing associated with earth pressure is the highest for a stiffness ratio of 3. The settlement moment at the footing level is higher for a lower stiffness ratio. The midspan moment is greater for a lower stiffness ratio  $K$  in the case of live load, dead load, and earth pressure. Moment caused by temperature loads at midspan is smaller for increased  $K$  values. Soil settlement moments are negligible at midspan for all values of  $K$  considered in our analysis.

The maximum midspan moment developed for hinged and fixed boundary conditions in a jointless bridge considered is nearly 50 percent lower than that in a jointed bridge. The effect of soil settlement is negligibly small for a hinged case, whereas the moment developed because of 1 in. of soil settlement in a fixed case at support is found to be about 20 percent of maximum moment at support. The effect of earth pressure is significant at the top of the abutment in the case of hinged condition and at the bottom of the abutment in case of a fixed condition. The effect of braking forces in both hinged and fixed jointless bridges is small compared with the maximum moments.

### FURTHER STUDY

The analytical data generated for single-span jointless bridges will be compared with the field data. A simple equivalent beam design model with rotational and translation spring constants is being developed for a portal frame. Equivalent rotational and translation spring constants will be arrived at considering the soil stiffness, foundation type, and integral bridge stiffness  $K$ . The equivalent beam model indicated in Figure 13 will be solved for a general loading to determine end moments. The beam model would be handy for practicing engineers. The merits and demerits of having an internal hinge between the superstructure and substructure will have to be assessed. The parametric study of two- and three-span bridges with different boundary conditions is being performed by varying the abutment/pier heights, type of foundation, soil conditions, and

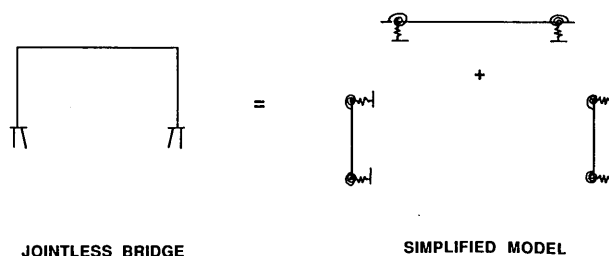


FIGURE 13 Simplified model for jointless bridge.

temperature variations. Length and tolerable movement limits will be established using the data from the parametric study and field.

## ACKNOWLEDGEMENTS

The research project was sponsored by the West Virginia Department of Highways and FHWA, U.S. Department of Transportation. Their financial support and suggestions are gratefully acknowledged.

## REFERENCES

1. Klaiber, W. F., et al. *NCHRP Report 293: Methods of Strengthening Existing Highway Bridges*. TRB, National Research Council, Washington D.C., 1987.
2. Dagher, J. H., et al. Analytical Investigation of Slab Bridges with Integral wall Abutments. In *Transportation Research Record 1319*, TRB, National Research Council, Washington, D.C., 1991, pp. 115-125.
3. Purvis, R. L., and R. H. Berger. Bridge Joint Maintenance. In *Transportation Research Record 399*, TRB, National Research Council, Washington, D.C., 1983.
4. Wolde-Tinsae, A. M., et al. Performance and Design of Jointless Bridge. *FHWA Final Report*. Department of Civil Engineering, University of Maryland, June 1987.
5. Burke, M. P. Integral Bridges: Attributes and Limitations. In *Transportation Research Record 1393*, TRB, National Research Council, Washington, D.C., 1993, pp. 1-8.
6. Burke, M. P. Integral Bridges. Presented at 69th Annual Meeting of the Transportation Research Board, Washington D.C., Jan. 1990.
7. Loveall, C. L. Jointless Bridge Decks. *Civil Engineering*, Vol. 55, No. 11, Nov. 1985, pp. 64-67.
8. Wasserman, E. P. Jointless Bridges. *Engineering Journal*, Vol. 24, No. 3, 1987, pp. 93-100.
9. Emanuel, J. H., and C. M. Taylor. Length-Thermal Stress Relations for Composite Bridges. *ASCE Journal of Structural Engineering*, Vol. 111, No. 4, April 1985.
10. Hulsey, J. L., and J. H. Emanuel. Environmental Stresses in Flexibly Supported Bridges. In *Transportation Research Record 664*, TRB, National Research Council, Washington, D.C., pp. 262-270.
11. Lam, P. I. Seismic Design of Highway Bridge Foundations. *FHWA Report RD-86/102*. FHWA, U.S. Department of Transportation, 1986.
12. *Standard Specifications for Highway Bridges*, 14th ed. AASHTO, Washington, D.C., 1989.
13. Hayden, G. A., and M. Barron *The Rigid-Frame Bridge*. John Wiley and Sons, New York, 1950.
14. Kleinlogel, A. *Rigid Frame Formulas*. Frederik Ungar Publishing Co., New York, 1964.
15. Greimann, L. F., et al. *Pile Design and Tests for Integral Abutment Bridges*. Iowa DOT Project 273, Iowa State University, Dec. 1987.
16. Ghali, A., and R. Favre. *Concrete Structures: Stresses and Deformations*. Chapman and Hall, New York, 1986.
17. ANSYS. *Engineering Analysis System User's Manual*. Swanson Analysis Systems, Inc., Houston, Pa., 1987.

---

*Publication of this paper sponsored by Committee on Steel Bridges.*